High-order harmonic generation from graphene: Strong attosecond pulses with arbitrary polarization

Stian Astad Sørngård,* Sigrid Ina Simonsen,† and Jan Petter Hansen
Department of Physics and Technology, University of Bergen, N-5007 Bergen, Norway
(Received 23 November 2012; published 3 May 2013)

We explore high-order harmonic generation (HHG) from a graphene sheet exposed to intense femtosecond laser pulses based on the Lewenstein model. It is demonstrated that the HHG cutoff frequency increases with graphene size up to the classical limit for distant diatomic systems. In contrast to two-center systems, the cutoff frequency remains constant with increasing power of the harmonics as the graphene diameter extends beyond maximal electron excursion. It is shown that the extended nature of the graphene sheet allows for strong HHG signals at maximum cutoff for linearly as well as circularly polarized laser pulses, the latter opening for generation of strong circularly polarized attosecond pulses.

DOI: 10.1103/PhysRevA.87.053803 PACS number(s): 42.65.Ky, 33.20.Xx, 81.05.ue

High-order harmonic generation (HHG) refers to the nonlinear process of creation of very high overtones of an intense laser pulse with central frequency ω_0, which interacts with a dilute gas of atoms or molecules. The realization of laser intensities beyond 10^{14} W/cm^2 paved the way for theoretical studies [1,2] and experiments [3–5] on HHG from a gas of atoms in the early 1990s. Now, after about 20 years of intense HHG research, the three-step model [6] describing HHG within a single-atom picture is well established: The atom (i) ionizes, (ii) gains energy when accelerated by the electric field in the continuum, and (iii) eventually recombines with the ion emitting a photon at odd multiples of the driving-field frequency. Since a single excursion and recombination of an electron takes place within one-half optical cycle, the generated HHG photons define a coherent attosecond high-frequency laser pulse which is a unique tool for probing and imaging of ultrafast dynamics [7–9]. In laser-based imaging the HHG spectra have been used for tomographic reconstruction of molecular orbitals with ångström spatial resolution [10–12].

In recent years HHG following interaction with molecules has received particular attention. First, it has been shown that ionization at one molecular center and recombination at another allows for larger maximum harmonic frequencies [13,14]. Second, the two-center structure allows for the generation of attosecond pulses with elliptical polarization as well as even harmonics if the inversion symmetry is broken [15,16]. It has been shown theoretically that a preprepared molecular medium can be used to produce controlled secondary attosecond pulses, when exposed to a seed attosecond XUV pulse [17]. In addition, the study of HHG has been advancing towards molecules of increasing complexity such as benzene rings [18], fullerenes [19], and carbon nanotubes [20], including the investigation of symmetry properties essential for the selective generation of high-order harmonics.

The realization of graphene [21], a two-dimensional monolayer of carbon atoms, has received explosive interest in the last decade due to its extraordinary physical properties such as its superior strength and electronic conductivity. What was for years believed to be nothing but a theoretical toy model of a carbon allotrope is today considered to be a new paradigm in condensed-matter physics [22]. The ordered structure of the HOMO p_z-like orbitals of graphene makes it particularly interesting for HHG since the classical three-step model here allows for a large number of atomic pairs of sites for ionization and recombination for linearly as well as for circularly polarized driving laser pulses. This may generate strong attosecond pulses with tunable polarization, two features which are difficult to obtain when HHG originates from an unordered molecular gas.

Thus, in this paper we perform a numerical simulation of HHG from graphene within the strong-field approximation (SFA). We perform numerical calculations for one- and two-dimensional lattice structures and investigate the impact of the dimensionality on the harmonic power spectra. The calculations are carried out for laser light with various linear polarization angles with respect to the graphene sheet arranged in the xy plane and for a circularly polarized laser in the plane of the atomic sites. Atomic units, where m_e, $\hbar$, and e are scaled to unity are used throughout unless stated otherwise. The model system is illustrated in Fig. 1, which shows the HOMO p_z orbitals defining a honeycomb lattice (comprising hexagonal cells). A (red) laser pulse is schematically propagating through the graphene sheet and interacting with a number N of atomic graphene sites. As a result of this interaction, a possible trajectory of an electron ionized at one site and recombining at another site is highlighted.

The HHG power spectrum of photon frequencies ω_0 propagating in the $\mathbf{n}$ direction, when cast into the velocity form, reads

$$S_{\mathbf{n}}(\omega) = \left| \mathbf{n} \cdot \left(\int_{-\infty}^{\infty} dt [e^{i\omega t} \langle \Psi(t) | \mathbf{p} | \Psi(t) \rangle^{\mathrm{SFA}}] \right) \right|^2, \qquad (1)$$

where the superscript SFA denotes that the ionized wave function is calculated in the SFA [23,24]. This particular form of the power spectrum is the one that relates directly to the harmonic field from a solution of the Maxwell equations [25]. To describe the wave function we adopt a simple one-electron multicenter model of the bound (initial) state Ψ_b in graphene by a coherent sum of atomic orbitals distributed on a honeycomb

*stian.sorngard@ift.uib.no
†sigrid.simonsen@ift.uib.no

lattice:

$$\Psi_{\rm b}(\mathbf{r},t) = \frac{1}{\sqrt{N}} \sum_{j}^{N} \psi(\mathbf{r}_j) e^{-i\varepsilon_0(t-t_0)}. \quad (2)$$

Here ε_0 can be taken as the (negative) ionization potential of graphene, and Gaussian-type orbitals are employed to describe each site-specific wave function, $\psi(\mathbf{r}_j) = a_j r_{j_x}^{k_j} r_{j_y}^{l_j} r_{j_z}^{m_j} e^{-\alpha(\mathbf{r}-\mathbf{R}_j)^2}$. The results depend very weakly on the detailed shape of the site functions so we limit the present investigation to a single Gaussian-type p_z orbital on each site, i.e. $k_j = l_j = 0$, and $m_j = 1$, with $\alpha = 1$.

In a perturbative approach it is well known that the final state, as well as the results, is sensitive to the choice of gauge [24]. The length and velocity gauges, where the interaction terms are given by $\mathbf{E}\cdot\mathbf{r}$ and $\mathbf{A}\cdot\mathbf{p}$, respectively, are both widely used in the literature. For extended systems, we note here that the length gauge results in a nonphysical origin dependence of the spectra with no upper limit of the cutoff frequency as the maximum distance between two site atoms becomes increasingly large [26,27]. We therefore describe the ionization in the velocity gauge, which, in contrast, gives a cutoff behavior for two atoms with increasing internuclear distance $\mathbf{R}$, in agreement with exact calculations. The ionized electron states are then described by Volkov waves,

$$\Psi_{\rm c}(\mathbf{r},t) = \left(\frac{1}{2\pi}\right)^{3/2} e^{i\mathbf{k}\cdot\mathbf{r} - iS(k,t,t_0)}, \quad (3)$$

where $S(k,t,t_0) = \frac{1}{2}\int_{t_0}^{t} dt'[\mathbf{k}+\mathbf{A}(t')]^2$ can be interpreted as the classical action of the field on the ejected electron. The expectation value of the momentum operator is readily expressed as

$$\langle\Psi(t)|\mathbf{p}|\Psi(t)\rangle^{\rm SFA} \approx -{\rm Re}\left\{\left(\frac{1}{2\pi}\right)^3 \int_0^t dt' e^{i\varepsilon_0(t-t')} \int d^3k e^{-iS(k,t,t')} \left[\int d^3r e^{-i\mathbf{k}\cdot\mathbf{r}} \mathbf{A}(t')\cdot\mathbf{p}\Psi_{\rm b}(\mathbf{r})\right]\left[\int d^3r \Psi_{\rm b}^*(\mathbf{r})\nabla e^{i\mathbf{k}\cdot\mathbf{r}}\right]\right\}, \quad (4)$$

where Ψ is the total wave function. The first and the second expression enclosed by square brackets is the amplitude for ionization to the Volkov state $|\mathbf{k}\rangle$ at time t', and the amplitude for recombination at a later time t, respectively. The k integral is evaluated by the stationary phase method. Test calculations have also been performed to ensure that this method gives, in general, comparable results to exact integral calculations. The driving laser pulse is modeled by a six-cycle plane wave with central frequency $\omega_0 = 0.057$ a.u. ($\lambda = 800$ nm) and amplitude $E_0 = 0.114$ a.u. ($I_{\rm peak} = 4.6\times10^{14}$ W/cm^2) modulated by a trapezoidal envelope. In the following we discuss results originating from interaction with a linearly polarized field, where the polarization vector of the pulse is tiled at angle θ with respect to the z axis. Subsequently, the case of a circularly polarized field in the plane of the honeycomb lattice modeling graphene is presented.

In Fig. 2 we compare the cutoff of the harmonic spectrum for one- and two-dimensional structures interacting with a linearly polarized field with $\theta = 45^\circ$ as a function of their diameter in the x direction. The figure compares results for a diatomic system, a multiatomic string, and a graphene sheet. The results of Moreno *et al.* and Bandrauk *et al.* [14,28] implied a maximum cutoff law for diatomic systems, $N_{\rm max} = (I_p + 8U_p)/\omega_0$, where I_p is the ionization potential and U_p is the ponderomotive energy. The field parameters applied in our work give a maximum harmonic order of $N_{\rm max} = 149$, which is in fairly good agreement with the maxima in Fig. 2.

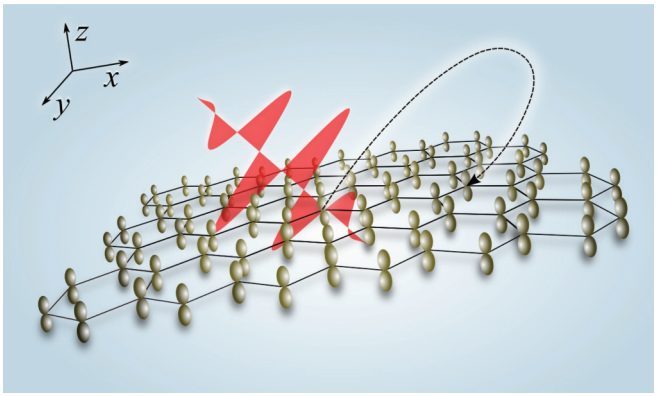

FIG. 1. (Color online) Artist's impression of graphene exposed to a linearly polarized laser pulse. The graphene layer is modeled by hydrogenic p_z orbitals distributed on a honeycomb lattice in the xy plane, and the polarization vector of the laser pulse is tilted with respect to the z axis. The trajectory illustrates the situation in which the ionized electron recombines with another atom in the lattice.

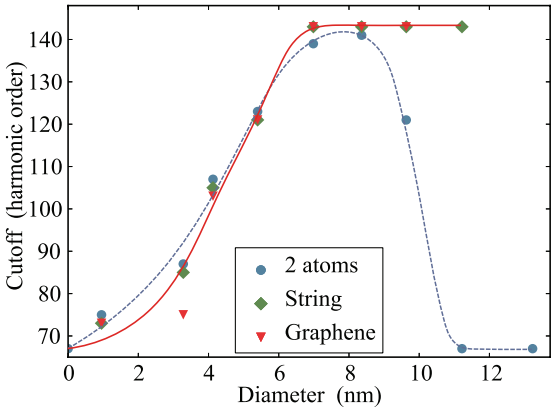

FIG. 2. (Color online) The harmonic spectrum cutoff as a function of the diameter of the focus area for a linearly polarized laser with polarization angle $\theta = 45^\circ$ for graphene [(red) triangles], a multiatom string along the x axis [(green) diamonds], and a two-atom string along the x axis [(blue) circles]. See the text for a more detailed description. Solid and dashed lines are plotted simply to guide the eye.

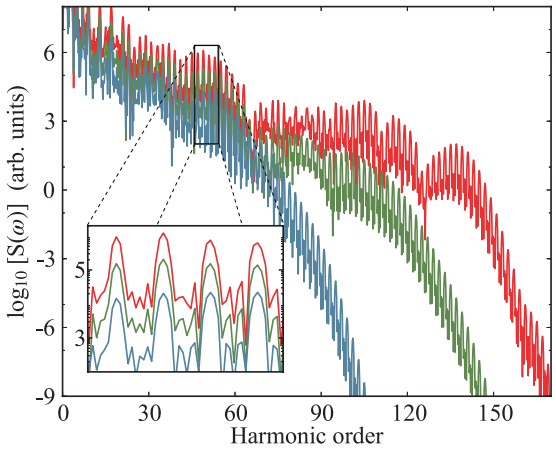

FIG. 3. (Color online) HHG power spectrum as a function of the harmonic order for a circular graphene sheet of 348 atoms [bottom (blue) line], 954 atoms [middle (green) line], and 2918 atoms [top (red) line] exposed to a linearly polarized laser. Inset: Closeup of the spectra. The polarization angle of the laser field is $\theta = 45^\circ$.

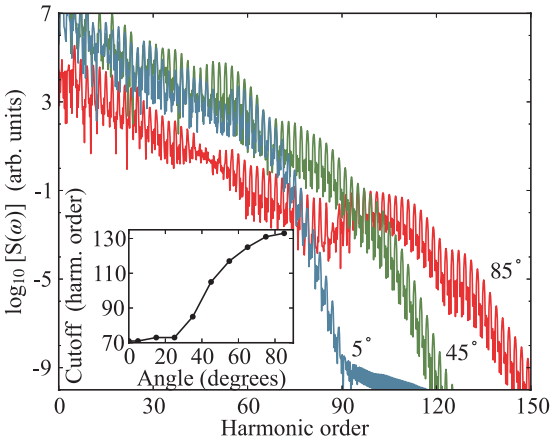

FIG. 4. (Color online) HHG power spectrum as a function of the harmonic order for a circularly shaped graphene layer composed of 552 atoms, with a diameter of 4.1 nm. The spectrum is plotted for three polarization angles of the linearly polarized field: 5° (blue line), 45° (green line), and 85° (red line). Inset: Cutoff as a function of the polarization angle.

Thus, atoms situated at the ideal interatomic distance in the x direction for classical ionization and recombination give rise to the same cutoff level for all three systems. For system diameters exceeding this ideal limit, the cutoff level for the diatomic system decreases until the spectrum is identical to the spectrum from two isolated atoms. In contrast, the cutoff frequency of the molecular string and the graphene sheet remain constant for increasing diameter. These systems support intermediate sites corresponding to optimal classical excursion.

In Fig. 3 we plot and compare the harmonic spectra from a graphene sheet with 348, 954, and 2918 atoms, which display the sensitivity of cutoff frequency on system size. The inset highlights the spectrum of odd harmonics around order ∼55. Most important is the observation that the intensity increases with the number of atoms. Thus, a stronger signal strength at cutoff is obtained from graphene sheets when the system size exposed to the laser pulse increases. In particular, this effect would yield a substantial enhancement of the signal power from an extended atomic structure compared to diatomic systems.

The sensitivity of the cutoff region to the polar angle θ between the z axis and the plane set up by the electric field deserves closer attention. In Fig. 4 we show harmonic power spectra for three choices of this angle for a fixed number of atoms. We observe an increasing cutoff with increasing angle. The dependence of the cutoff on the angle is depicted in the inset. Initially and up to 20° the dependence is very weak, which can be attributed to the dominant process of ionization and recollision at the same atom. At larger angles, a greater number of classical recombination sites opens up, and consequently the harmonic order grows. We note, however, that the stationary phase approximation breaks down at $\theta = 90^\circ$ for p_z orbitals. The apparently weaker harmonic spectrum at 85° is simply a result of this malfunction in the approximation, and it must be emphasized that exact calculations do not show such a deviation.

An important feature with our graphene model is the ability to generate strong high-order harmonics from circularly polarized laser pulses. To remain at a model level, here we replace p_z with s states and consider circularly xy polarized laser pulses propagating in the direction perpendicular to the graphene plane [29]. The upper panel in Fig. 5 displays the cutoff as a function of the number of atoms in the honeycomb lattice. A behavior of the cutoff and a strength similar to those for linearly polarized light are found (cf. Fig. 2). Again, the

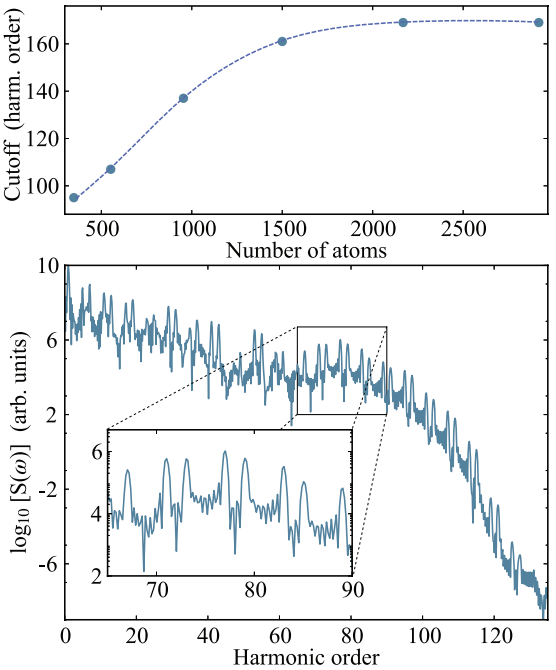

FIG. 5. (Color online) Top: Cutoff as a function of the number of atoms in a graphene sheet modeled by s orbitals exposed to a circularly polarized laser in the xy plane. Bottom: Power spectrum corresponding to 348 atoms. Inset: Closeup demonstrating the twin-peak power spectrum that characterizes the hexagonal lattice.

three-step model explains the phenomenon. For a dilute gas of molecules or atoms, the probability of recombining with the parent atom, or another atom, after an excursion in the continuum along a rotating electric field is almost 0. When the atoms are ordered in a regularly (infinite) flat molecule the recombination sites are of the same order as for the linearly polarized case. Thus, graphene as a target medium may be used to generate strong circularly polarized attosecond laser pulses.

The lower panel in Fig. 5 shows the power spectrum from 348 atoms arranged as graphene. This spectrum differs from the other spectra presented in that it exhibits a twin-peak structure. The twin peaks appear in accordance with the selection rule $6j \pm 1$ ($j = 0, 1, \ldots$) first demonstrated by Alon *et al.* [30] and Baer *et al.* [18]. In these works the selection rules, for HHG spectra in general and for benzene rings aligned in the polarization plane of circular laser pulses in particular, are derived. Although the honeycomb grid structure is more involved, Fig. 5 clearly demonstrates that the selection rules in fact are those of a single hexagonal cell provided that the cells are symmetrically oriented with respect to the origin.

An experimental setup for testing the present findings will require a strong driving laser field to penetrate a large number of graphene sheets in order to produce strong high-order harmonic signals. This can be achieved in two ways: first, by using gas-phase graphene sheets kept aligned by a dynamic laser system coupled to the driving laser. Robust dynamical alignment of large gas-phase molecules has been demonstrated, e.g., in [31]. Alternatively, one can envision that a large number of graphene sheets can be stacked based on the rapidly evolving solution-phase technique with controlled stacking [32]. In both cases the HHG signal will become amplified similarly to that in HHG experiments with gas-phase atoms, with the additional benefit of higher photon frequencies and tunable polarization. A possible challenge will be to avoid heating and potentially damaging the graphene sheets, e.g., as demonstrated in [33]. We believe that shorter femtosecond pulse durations of only a few optical cycles may reduce this effect.

In summary, the present work has shown that graphene may generate more intense harmonic signals than gas-phase atoms or molecules and serve as a useful tool for selective harmonic generation when exposed to an intense driving laser field. This is established based on the Lewenstein model in combination with the simplest possible model representation of the HOMO state of graphene. Furthermore, the focal area spanned by a propagating circularly polarized laser pulse contains a large number of atoms available for recombination with ionized electrons. This mechanism generates strong HHG signals also from a circularly polarized driving laser, which may generate strong attosecond pulses with circular polarization.

The authors thank Morten Førre, Adam Etches, and Lars Boyer Madsen for thorough and illuminating discussions. This research was supported by the Research Council of Norway (RCN), the Bergen Research Foundation (Norway), and the Norwegian Metacenter for Computational Science (NOTUR).

[1] A. L'Huillier, K. J. Schafer, and K. C. Kulander, J. Phys. B **24**, 3315 (1991).
[2] J. L. Krause, K. J. Schafer, and K. C. Kulander, Phys. Rev. Lett. **68**, 3535 (1992).
[3] K. Miyazaki and H. Sakai, J. Phys. B **25**, L83 (1992).
[4] J. J. Macklin, J. D. Kmetec, and C. L. Gordon, Phys. Rev. Lett. **70**, 766 (1993).
[5] A. L'Huillier and P. Balcou, Phys. Rev. Lett. **70**, 774 (1993).
[6] P. B. Corkum, Phys. Rev. Lett. **71**, 1994 (1993).
[7] J. Itatani, J. Levesque, D. Zeidler, H. Niikura, H. Pepin, J. C. Kieffer, P. B. Corkum, and D. M. Villeneuve, Nature **432**, 867 (2004).
[8] A. Fohlisch, P. Feulner, F. Hennies, A. Fink, D. Menzel, D. Sanchez-Portal, P. M. Echenique, and W. Wurth, Nature **436**, 373 (2005).
[9] F. Krausz and M. Ivanov, Rev. Mod. Phys. **81**, 163 (2009).
[10] M. Lein, J. Phys. **40**, R135 (2007).
[11] S. Haessler, J. Caillat, W. Boutu, C. Giovanetti-Teixeira, T. Ruchon, T. Auguste, Z. Diveki, P. Breger, A. Maquet, B. Carre *et al.*, Nat. Phys. **6**, 200 (2010).
[12] E. V. van der Zwan and M. Lein, Phys. Rev. Lett. **108**, 043004 (2012).
[13] T. D. Donnelly, T. Ditmire, K. Neuman, M. D. Perry, and R. W. Falcone, Phys. Rev. Lett. **76**, 2472 (1996).
[14] A. D. Bandrauk, S. Chelkowski, H. Yu, and E. Constant, Phys. Rev. A **56**, R2537 (1997).
[15] C. B. Madsen and L. B. Madsen, Phys. Rev. A **74**, 023403 (2006).
[16] T. Kreibich, M. Lein, V. Engel, and E. K. U. Gross, Phys. Rev. Lett. **87**, 103901 (2001).
[17] M. Førre, E. Mével, and E. Constant, Phys. Rev. A **83**, 021402(R) (2011).
[18] R. Baer, D. Neuhauser, P. R. Ždánská, and N. Moiseyev, Phys. Rev. A **68**, 043406 (2003).
[19] G. P. Zhang, Phys. Rev. Lett. **95**, 047401 (2005).
[20] O. E. Alon, V. Averbukh, and N. Moiseyev, Phys. Rev. Lett. **85**, 5218 (2000).
[21] K. S. Novoselov, A. K. Geim, S. V. Morozov, D. Jiang, Y. Zhang, S. V. Dubonos, I. V. Grigorieva, and A. A. Firsov, Science **306**, 666 (2004).
[22] A. K. Geim and K. S. Novoselov, Nat. Mat. **6**, 183 (2007).
[23] L. V. Keldysh, Sov. Phys. JETP **20**, 1307 (1964).
[24] H. R. Reiss, Phys. Rev. A **22**, 1786 (1980).
[25] J. C. Baggesen and L. B. Madsen, J. Phys. B **44**, 115601 (2011).
[26] C. C. Chirilă and M. Lein, Phys. Rev. A **73**, 023410 (2006).
[27] J. Chen and S. G. Chen, Phys. Rev. A **75**, 041402(R) (2007).
[28] P. Moreno, L. Plaja, and L. Roso, J. Opt. Soc. Am. B **13**, 430 (1996).
[29] The Gaussian-type s and p_z orbitals representing the site functions in the graphene molecule are expected to yield qualitatively the same results. Within the stationary phase method the p_z orbital gives vanishing HHG spetra for circular polarized light in the xy plane.

[30] O. E. Alon, V. Averbukh, and N. Moiseyev, Phys. Rev. Lett. **80**, 3743 (1998).

[31] S. S. Viftrup, V. Kumarappan, S. Trippel, H. Stapelfeldt, E. Hamilton, and T. Seideman, Phys. Rev. Lett. **99**, 143602 (2007).

[32] K. Yu, P. Wang, G. Lu, K.-H. Chen, Z. Bo, and J. Chen, J. Phys. Chem. Lett. **2**, 537 (2011).

[33] A. Roberts, D. Cormode, C. Reynolds, T. Newhouse-Illige, B. J. LeRoy, and A. S. Sandhu, Appl. Phys. Lett. **99**, 051912 (2011).